

# Experimental wireless channel analysis between 1 and 40 GHz in an indoor NLoS corridor environment

Juan Pascual-García<sup>1</sup>, Maria-Teresa Martinez-Ingles<sup>2</sup>, Davy P Gaillot<sup>3</sup>, José-María Molina-García-Pardo<sup>1</sup>, Esteban Egea-López<sup>1</sup>

<sup>1</sup> Universidad Politécnica de Cartagena, UPCT, Dpto. Tecnologías de la Información y las Comunicaciones, Cartagena, Murcia, Spain, juan.pascual@upct.es, josemaria.molina@upct.es, esteban.egea@upct.es

<sup>2</sup> Center of Defense, CUD, San Javier Air Force Base, Ministerio de Defensa-Universidad Politécnica de Cartagena, Santiago de la Ribera (Spain), mteresa.martinez@ cud.upct.es

<sup>3</sup> University of Lille, IEMN/TELICE, Villeneuve d'Ascq, France, davy.gaillot@univ-lille1.fr

**Abstract**—This work presents an analysis of the wireless channel based on a measurement campaign performed from 1 GHz to 40 GHz in an Non-Line-of-Sight (NLoS) indoor corridor environment. The delay characteristics and path loss parameters are estimated for different sub-bands. The NLoS values are compared with Line-of-Sight (LoS) results extracted from the same measurement campaign. The channel sounder is based on a Vector Network Analyzer, one linear positioning system and Optical-Radio transceivers. The positioning system allows the measurement of MIMO channel transfer functions. These functions are measured without distance limitation thanks to the fiber-optic system.

**Index Terms**— propagation, measurement, indoor, 5G.

## I. INTRODUCTION

Several bands between 1 and 40 GHz have been selected to deploy the new 5G mobile communication systems and other wireless ultra-high data rate systems. Particularly, in the last World Radio Communication Conference (WRC) held in 2015, the 24.25-27.5 GHz, 31.8-33.4 GHz and 37-40.5 GHz bands were fixed to locate the future 5G systems above 6 GHz [1]. Below 6 GHz we can also find different bands, as for example, the band between 3.4-3.8 GHz in Europe, the 3.4-3.6 and 4.8-5 GHz bands selected by China, the 3.4-3.7 GHz band in Korea, the 3.6-4.2, and 4.4-4.9 GHz bands awarded in Japan. Furthermore, in USA the 3.55–3.7 GHz band has been selected for a new Citizens Broadband Radio Service (CBRS). This year the final frequency bands will be defined in the WRC'19.

There exist few works that address a comparison of all mentioned bands under NLoS conditions. In [2] the path loss, angle and delay characteristics are studied using statistical simulations at 28 GHz under both LoS and NLoS conditions. Measurements in NLoS environments are found in [3] where a channel sounder was used to analyze the directional properties at 26 GHz; in [4] several bands between 800 MHz and 37 GHz were measured to obtain a path loss model for NLoS microcellular environments. In this work, we have measured MIMO transfer functions in the complete band between 1 and 40 GHz in a NLoS indoor environment; this way we can extract the transfer functions and the channel parameters from the whole band and from

the selected bands without limitation, allowing a complete characterization of the channel. This work is the continuation of the work [5], where the analysis of the wireless channel was carried out in the same band in a LoS indoor scenario.

This paper is organized as follows. Section II describes the propagation environment. Section III shows the used channel sounder. The Power Delay Profile (PDP), relative received power, and RMS (Root Mean Square) delay spread are shown in section IV. Finally, the conclusions are explained in section V.

## II. PROPAGATION ENVIRONMENT

The scenario for the measurements is a corridor of one building of the Universidad Politécnica de Cartagena as is showed in Fig.1. The dimensions of the corridor and the transmitter (Tx) locations are depicted in Fig. 2; the ceiling height is 4.13 m. and the width of the corridor 2 m. The Tx locations are uniformly distributed along the corridor; the separation between two consecutive locations is 0.8 m., except for the last position where a 0.4 m separation was chosen.

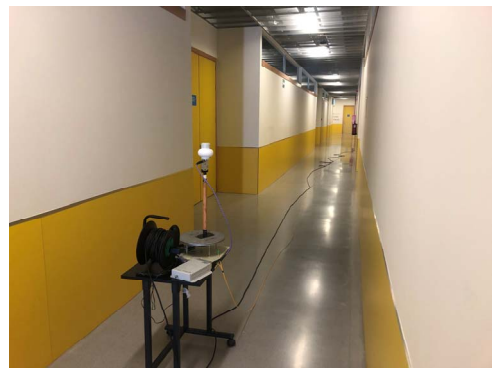


Figure 1. Photo of the measured corridor and the transmitter antenna.

One position inside a room, that faces the corridor, is selected for the receiver and it is marked in Fig. 2 as “ULA Rx<sub>1x5</sub>”. As seen in Fig.2 some Tx locations in the corridor, and all the locations placed inside the room, are in LoS.

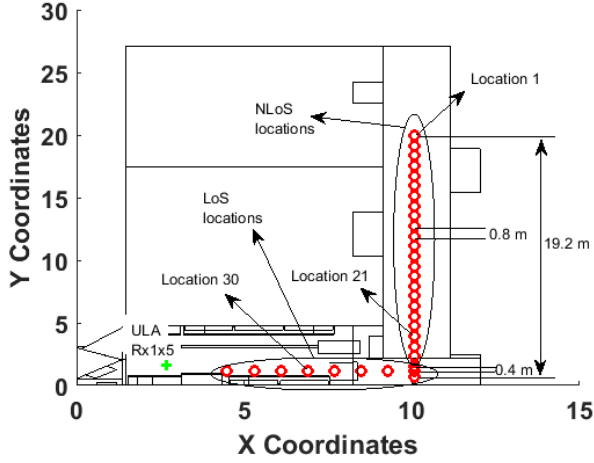


Figure 2. Top view scheme of the scenario. The receiver represented with a green cross is the ULA, each transmitter is a single antenna represented with a red circle.

### III. CHANNEL SOUNDER

The channel sounder is based on a commercial vector network analyzer (VNA) (Rohde and Swartz ZVA 10 MHz - 67 GHz, [6]), and a radio over fiber (RoF) link (EMCORE, Optiva OTS-2, 40 GHz [7]). To perform a wideband measurement and to collect the effect of all propagation mechanisms ultra-wideband omnidirectional antennas were selected at the Tx and Rx. The antennas are Steatite Q-PAR, 0.8-40 GHz [8].

The receiver subsystem was directly connected to the VNA and it is mounted over a linear positioner, simulating 5 virtual positions, regularly spaced 3 mm. The signal radio frequency (RF) of the VNA was brought to the Tx antenna making use of the radio over fiber link (more details are giving in [5]). This channel sounder allows the measure of the frequency response  $H(f)$ . The number of frequency points in the complete band was set to 16000, therefore avoiding the aliasing effect in all measurements.

The output power of the VNA was set to -25 dBm to avoid the saturation of the fiber optic system amplifiers and the intermediate frequency bandwidth was set to 1000 Hz. The previous value permitted a good trade-off between the measurement time and dynamic range. During the measurements, nobody was neither in the corridor nor in the room in order to guarantee stationarity conditions.

### IV. POWER DELAY PROFILE, RELATIVE RECEIVED POWER, AND RMS DELAY SPREAD

The Power Delay Profile, (PDP) was computed by averaging spatially the channel impulse response,  $|h(t,\tau)|^2$  over the 5 receiver positions for each Tx location:

$$P(\tau) = \overline{|h(t,\tau)|^2} \quad (1)$$

Fig. 3 depicts the PDP for three representative Tx locations (see Fig. 2). The hanning window was applied in all cases. Location 1 corresponds to a clearly NLoS situation, the power of the components is around 15 dB above the

noise floor. Location 21 is NLoS, but the main components are obstructed only by the wall and cupboard of the room where the Rx is placed, thus the attenuation is smaller than in the previous locations. Location 30 is a LoS situation and all main components are unobstructed.

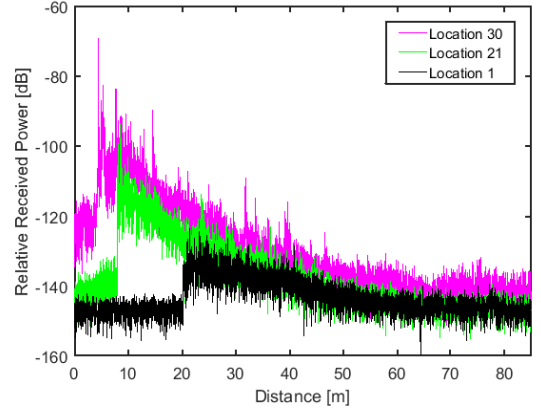


Figure 3. Full Bandwidth PDP for locations 30, 21 and 1.

It is interesting to analyze the components power at different bands in one NLoS location. Each band has a 2 GHz bandwidth and the central frequencies are: 2, 5, 10, 15, 20, 25, 30, 35, and 39 GHz. In Fig. 4 the PDP of bands centered at 2, 5 and 25 GHz show that above 25 GHz almost no components energy is collected when the Tx is in a NLoS location and relatively far from the receiver. From the analysis of the PDPs it is also shown that only noise is received for frequencies above 35 GHz in locations clearly in NLoS situations (from location 1 to 20).

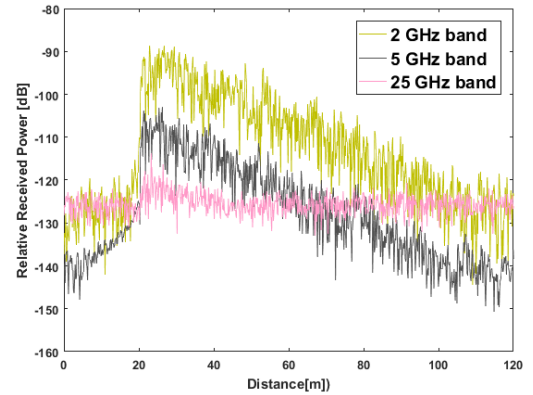


Figure 4. PDP for the bands centered at 2, 5, and 25 GHz for location 1.

The wideband relative received power can be obtained from the transfer function in frequency domain as:

$$P = \langle H(f) \rangle_f \quad (2)$$

Using the previous equation the received power for all bands has been estimated. The received power values corresponding to the ones where only noise is received are removed from the set. Once this operation is performed the 1-slope model has been calculated using the known equation:

$$P = P_0 + 10 \cdot n \cdot \log_{10}(d) \text{ (dB)} \quad (3)$$

Fig. 5 shows the relative received power for all bands, and their corresponding 1-slope models.

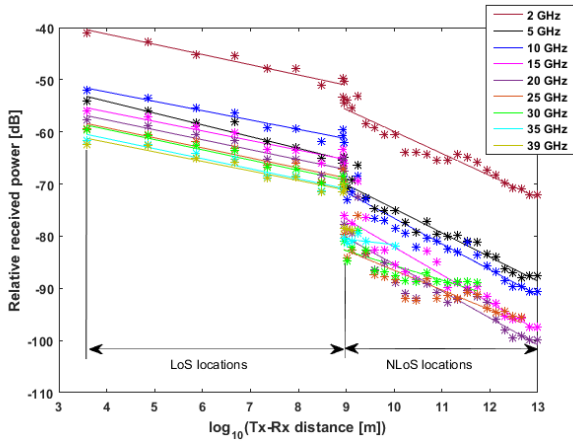


Figure 5. Relative received powers and 1-slope model for all bands.

The model parameters (slope and relative received power at 1 meter) are shown in table I.

TABLE I  
ONE-SLOPE MODEL FOR ALL SUB-BANDS

$f_0$ GHz	NLoS		LoS	
	$P_0$	$n$	$P_0$	$n$
<b>2</b>	-17.63	-4.22	-33.39	-1.96
<b>5</b>	-28.44	-4.62	-45.12	-2.25
<b>10</b>	-27.20	-4.93	-45.19	-1.78
<b>15</b>	-28.75	-5.33	-48.82	-1.83
<b>20</b>	-33.93	-5.14	-50.05	-1.90
<b>25</b>	-48.64	-3.78	-51.48	-1.92
<b>30</b>	-57.31	-2.82	-51.68	-1.95
<b>35</b>	-71.21	-1.03	-53.56	-1.92
<b>39</b>	-56.99	-2.40	-54.67	-1.82

The decay factor is above 4 in almost all cases for the NLoS situations; only the higher frequencies present lower values of “n” due to the absence of enough values with significant power to show the trend; only locations near the room present components above the noise floor at higher frequencies. In the LoS locations the decay factor is below 2 showing that reverberation effects are present even in locations inside a room when a door is open and in corridor locations with LoS.

The spread in the delay domain is usually represented by the RMS delay Spread. This parameter is defined as:

$$\sigma_\tau = \sqrt{\frac{\sum_k P(\tau_k) \tau_k^2}{\sum_k P(\tau_k)} - \left( \frac{\sum_k P(\tau_k) \tau_k}{\sum_k P(\tau_k)} \right)^2} \quad (4)$$

Fig. 6 shows the RMS delay spread for all sub-bands with respect the logarithm of the distance between Tx and Rx. Depending on the location, and therefore depending on the components power, and frequency band an appropriate

threshold has been used. The 1-slope model has also been obtained for the RMS. Negative values of the decay factor has been found for the higher frequencies whereas positive values seems to be more appropriate for the lower bands.

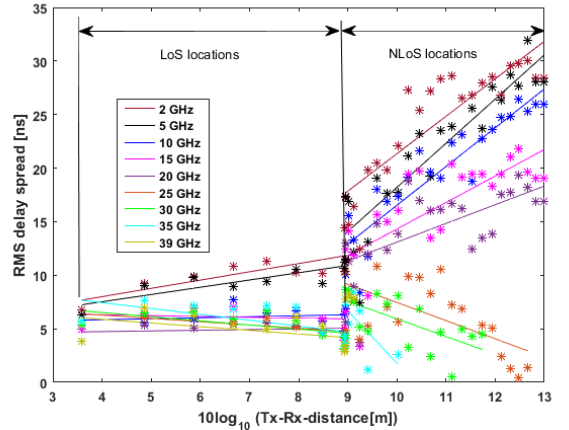


Figure 6. RMS and 1-slope model for all bands.

## V. CONCLUSIONS

The results have shown that for frequencies above 25 GHz almost no energy is received for Tx-Rx distances larger than 10 meters. The NLoS decay factor for all bands with enough data is above 4. The RMS in NLoS situations reaches values larger than 10 ns, higher frequencies show small values due to the presence of only few components above the threshold which produces very small RMS values.

## ACKNOWLEDGMENT

This work was supported by the Ministerio de Economía y Competitividad MINECO, Spain (TEC2016-78028-C3-2-P) and by the European FEDER funds.

## REFERENCES

- [1] World Radiocommunications Conference, “Resolution 238,” 2015.
- [2] T. Mantoro, M. A. Ayu and M. R. Nugroho, “NLOS and LOS of the 28 GHz bands millimeter-wave in 5G cellular networks,” *2017 International Conference on Computing, Engineering, and Design (ICCED)*, Kuala Lumpur, 2017, pp. 1-5.
- [3] M. Khalily, S. Taheri, P. Xiao, F. Entezami, T. A. Hill and R. Tafazolli, “26 GHz indoor wideband directional channel measurement and analysis in LoS and NLoS scenarios,” *12th European Conference on Antennas and Propagation (EuCAP 2018)*, London, 2018, pp. 1-5.
- [4] K. Kitao et al., “Path loss prediction model for 800 MHz to 37 GHz in NLOS microcell environment,” *2015 IEEE 26th Annual International Symposium on Personal, Indoor, and Mobile Radio Communications (PIMRC)*, Hong Kong, 2015, pp. 414-418.
- [5] M.-T. Martinez-Ingles, J. Pascual-García, D. P. Gaillot, C. Sanchis-Borras, J.-M. Molina-García-Pardo, “Indoor 1-40 GHz Channel Measurements,” *13th European Conference on Antennas and Propagation (EuCAP 2018)*, Krakow, 2019, pp. 1-5.
- [6] R&S Vector Network analyzer ZVA67
- [7] Optiva OTS-2 Series Microwave Band 50 MHz to 40 GHz Fiber Optic Links
- [8] Steatite Ultra-Wideband Omni-directional Antenna 0.8 to 40 GHz